catalysts

MDPI

Article

Photocatalytic Degradation of Diclofenac in Tap Water on TiO_2 Nanotubes Assisted with Ozone Generated from Boron-Doped Diamond Electrode

Daichuan Ma [1], Xianying Han [2], Xinsheng Li [1,3,*] and Daibing Luo [1,*]

[1] Analytical & Testing Center, Sichuan University, No. 29, Wangjiang Road, Wuhou District, Chengdu 610064, China; dcma@scu.edu.cn
[2] College of New Materials and Chemical Engineering, Beijing Institute of Petrochemical Technology, No. 19, North Qingyuan Road, Daxing District, Beijing 102617, China; hanxianying@bipt.edu.cn
[3] College of Computer Science, Sichuan University, No. 24, South Section 1, Yihuan Road, Wuhou District, Chengdu 610065, China
* Correspondence: lixinsheng@scu.edu.cn (X.L.); luodb@scu.edu.cn (D.L.)

Abstract: Degradation of pharmaceuticals in water by TiO_2 photocatalysis often suffers from low efficiency due to low activity and mass transfer limitation. In this work, diclofenac removal in tap water was performed by photocatalysis on TiO_2 nanotube growth on Ti mesh substrate assisted by ozone (O_3), which was generated from a hole-arrayed boron-doped diamond (HABDD) film electrode. The vertically oriented TiO_2 nanotubes were used as the heterogeneous photocatalyst. The HABDD, as a self-standing diamond electrode, was designed and custom-made by MWCVD technology. The microstructures and crystalline of the TiO_2 nanotubes and HABDD were characterized by a scanning electronic micrograph (SEM) and X-ray diffraction (XRD). Unlike other ozone generation methods, direct generation of ozone in the flowing water was applied in the photocatalysis process, and its effect was discussed. The diclofenac removal performance of the electrochemical-photocatalytic system was studied depending on O_3 generation efficiency, flowing rate, and the initial diclofenac concentration. The enhanced degradation effect from O_3 molecules on TiO_2 photocatalysis was attributed to the larger active surface area, the increased photo-generated charge separation rate, and the contact area of O_3. The degradation efficiency in the combined electrochemical-photocatalytic TiO_2/O_3/UV system was higher than that of the O_3/UV and TiO_2/UV routes individually. Furthermore, a theoretical calculation was used to analyze the TiO_2/O_3 interface in aqueous media in terms of the final energy. This system created an almost in situ feeding channel of oxidants in the TiO_2 photocatalysis process, thus increasing photocatalytic efficiency. This synergetic system is promising in the treatment of pharmaceuticals in water.

Keywords: TiO_2 nanotubes; ozone; photocatalysis; diclofenac degradation; boron-doped diamond

Citation: Ma, D.; Han, X.; Li, X.; Luo, D. Photocatalytic Degradation of Diclofenac in Tap Water on TiO_2 Nanotubes Assisted with Ozone Generated from Boron-Doped Diamond Electrode. *Catalysts* **2023**, *13*, 877. https://doi.org/10.3390/catal13050877

Academic Editors: Mingjun Jia and Xintong Zhang

Received: 18 April 2023
Revised: 6 May 2023
Accepted: 10 May 2023
Published: 12 May 2023

1. Introduction

The development of powerful and cost-effectively photocatalytic systems for the degradation of organics in water has attracted attention since it is of great importance for the protection of public health and the environment. TiO_2 photocatalyst, owing to its chemically inert, environmentally friendly, and low cost, has been extensively studied for the decomposition of varieties of pharmaceuticals in water [1,2]. In recent years, the degradation of diclofenac in municipal drinking water has been investigated by TiO_2 photocatalysis [3,4]. Diclofenac is a popular anti-inflammatory pharmaceutical drug, and its trace has been widely used around the world. The presence of diclofenac in environmental water has been found, and its degradation is a complicated problem [5]. Diclofenac is susceptible to photocatalysis degradation with complex mechanisms, depending on the method. Many by-products will be generated in the treatment processes, and drinking

water should be free from these compounds to minimize the unpredictable risk even with low concentrations. Therefore, developing new powerful treatment methods are required not only for diclofenac removal but also for the by-product's mineralization.

Currently, TiO_2 materials used for organic waste degradation in water are usually TiO_2 powders, films, or doped composites. Alternatively, TiO_2 nanotubes are ideal candidates in future environmental technologies due to their high areas and high adsorption ability. However, the relatively low utility efficiency of photo energy on TiO_2 is the main drawback when used in the photocatalytic oxidation of pollutants in water. Under this circumstance, combining TiO_2 nanotubes and Ozone (O_3) is an effective process for pharmaceutical mineralization in drinking and municipal water [6,7]. Ozone itself can quickly remove many organic compounds in water to some extent [8]. The use of O_3 in TiO_2 photocatalysis is helpful for the oxidation of organics with the advantage of boosting the reactions at room temperature since O_3 can capture the photo-generated electrons on the TiO_2 surface to form active radicals, thus achieving a cost-effective advanced oxidation process (AOP) effect [9,10]. In general, O_3 is produced from pure oxygen Sanders generators [5], which require special instruments or a pure oxygen supply to ensure continuous generation. However, ozone generated directly in the aqueous solution following TiO_2 photocatalysis has not been systematically investigated, which may demonstrate special properties in the synergetic $TiO_2/O_3/UV$ system from the larger reaction cross-section in homogeneous reactions.

In this work, we proposed an electrochemical system based on a hole-arrayed boron-doped diamond (HABDD) free-standing electrode as the ozone generator to feed the TiO_2 nanotubes photocatalysis process, which was used for the purification of diclofenac-containing tap water (Figure 1). Boron-doped diamond (BDD) film electrodes are promising for the electrochemical generation of ozone from tap water electrolysis at room temperature [11]. BDD materials have attracted attention since they are promising anodes in wastewater treatment due to their lower adsorption surface, highly anti-corrosion performance, low background current, and wide potential window. Direct generation of O_3 from BDD in tap water plays an important role in affecting the diclofenac degradation efficiency in liquid fluent reactors. Combining BDD electrochemistry and TiO_2 photocatalysis has been proven as an effective strategy for organics degradation in water [12,13]. The O_3 molecule, as a powerful oxidant, can capture the photo-generated electrons on TiO_2, producing highly active species to attack organics in water. In this system, an almost in situ feeding path was provided to further improve the photocatalytic efficiency.

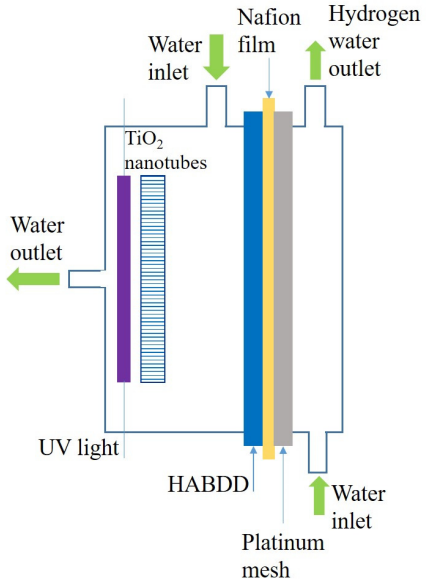

Figure 1. Schematic illustration of the electrochemical-photocatalysis system based on HABDD and TiO_2 nanotubes for diclofenac-containing tap water treatment.

2. Results and Discussion

2.1. HABDD Characterization

The SEM images of the HABDD surface and its inner structure are shown in Figure 2. The arrayed holes are equally distributed in the HABDD structure, forming squares by each four neighboring ones. The interval between each neighbored hole on the HABDD is about 2 mm (Figure 2a). Each hole has a diameter of about 0.5 mm (500 μm) with a depth of 1 mm, the same as the HABDD thickness (Figure 2b). All the substrate surfaces, including the planar surface on both sides and along the hole depth, are covered with the diamond phase. The HABDD has a uniform surface compacted with diamond microcrystals, as shown in Figure 2c. The reaction areas on the HABDD electrode are expanded from the plane surface to the sectional depth, which forms a three-dimensional reaction zone and raise the active sites in the electrode. The kinetics process of the 3D holey framework enables the ions to be efficiently transported to active sites buried deeply in the electrode.

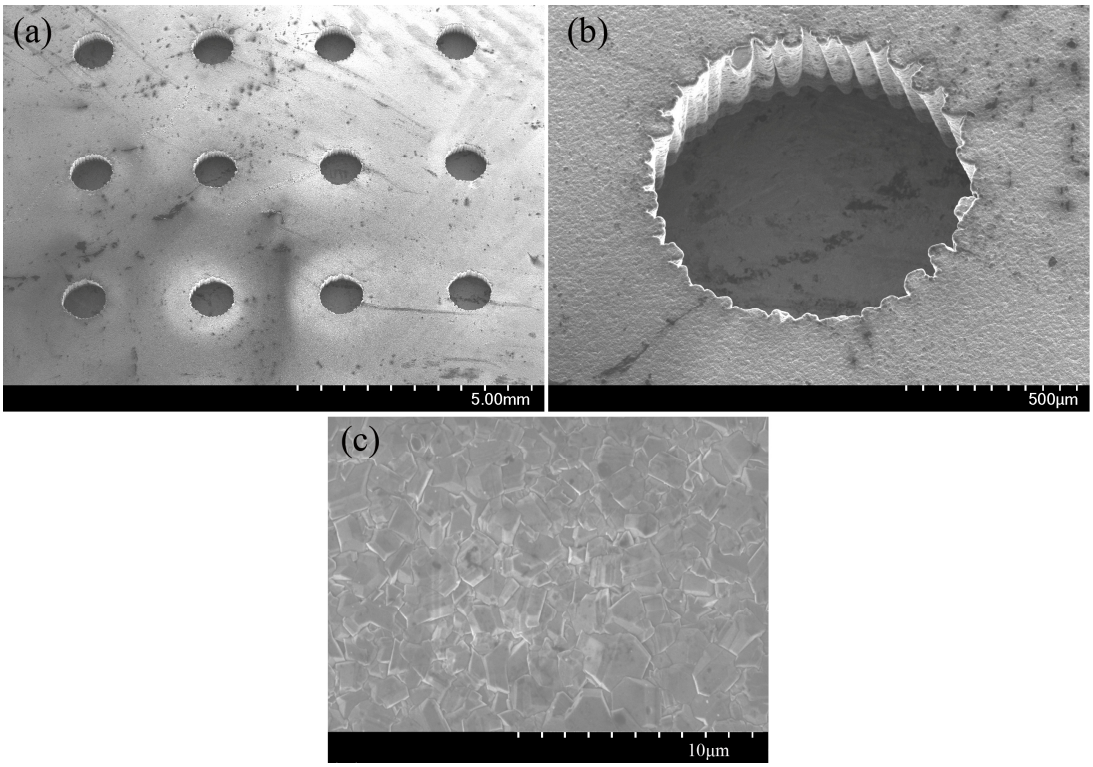

Figure 2. SEM graphs of (**a**) One side of the HABDD surface from the top view; (**b**) Insight of a micro hole; and (**c**) Morphology of the HABDD surface.

2.2. TiO_2 Nanotubes Characterization

A top view of the TiO_2 nanotube growth on the Ti mesh is shown in Figure 3a. The TiO_2 nanotubes formed on the Ti substrate are vertically aligned on the surface. The nanotubes have an internal diameter of about 60~100 nm, wall thickness of about 20 nm, and film thickness of about 10 μm. The nanotubes allow the photon absorption path length to exceed the electron transport distance along the nanotube length. The XRD results of the TiO_2 nanotubes and the Ti substrate are shown in Figure 3c. It can be seen the nanotubes were formed in anatase TiO_2 characterized by the featured diffraction peaks at 2θ of 25.5°, 38.1°, and 48.3°, which belong to the (101), (004), and (200) lattice facets of anatase TiO_2 phase. The TiO_2 nanotubes, with a larger surface area with a BET value of 269 m^2/g, could provide a more active reaction place for the photogeneration of electrons and holes for active radicals formation. In contrast with commercial P25 TiO_2, anatase TiO_2 nanotubes have a higher photocatalytic activity.

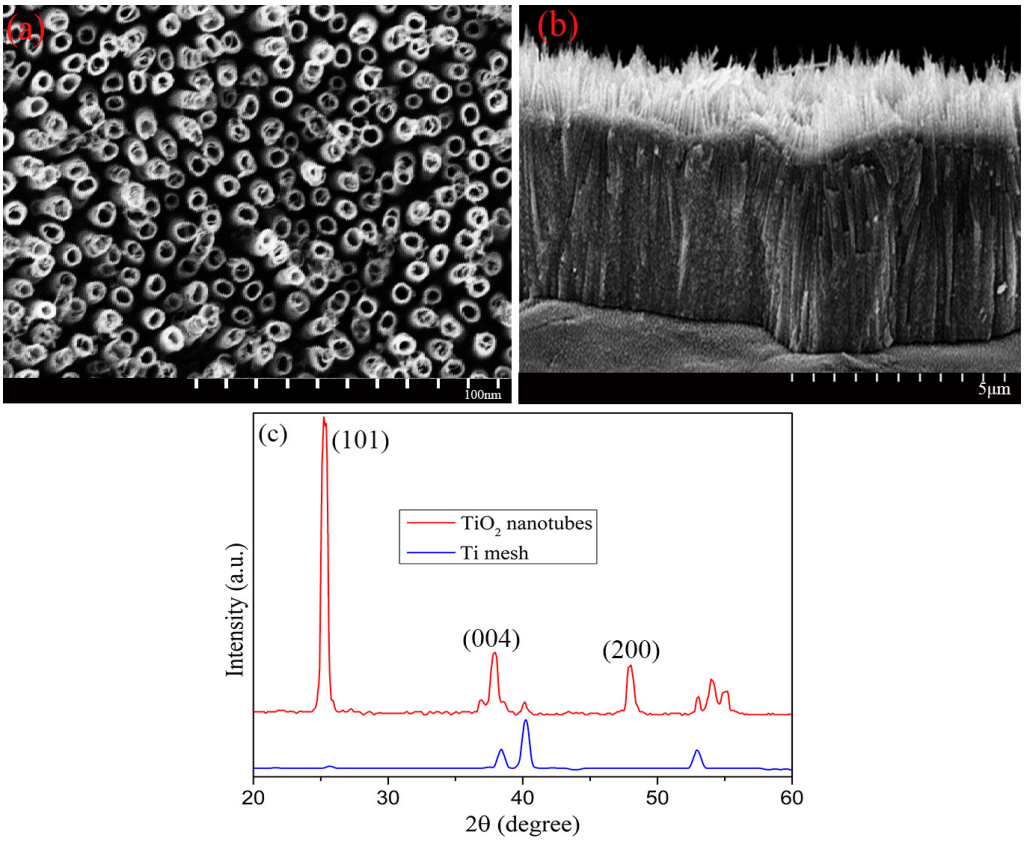

Figure 3. SEM images of the TiO_2 nanotubes on the Ti mesh from (**a**) up view and (**b**) side view. (**c**) XRD patterns of the TiO_2 nanotubes (red line) and Ti mesh substrate (blue line).

2.3. Ozone Generation Performance

The generated ozone in the tap water from 0.064 mg/L to 0.382 mg/L almost linearly with the applied current increased, ranging from 0.1 A to 0.5 A (Figure 4a). The production rate of ozone dissolved in the tap water was almost linear to the applied current. The continuous evolution of bubbles from tap water electrolysis will cause mechanical damage to conventional electrode materials. Therefore, mechanical durability is an urgent concern in ozone production from electrolysis, which can be reflected by the ozone production rate over working time. Fortunately, ozone could be continuously produced on the HABDD free-standing electrode after long-term durability (Figure 4b) due to the high stability of diamond materials. The concentrations of the ozone were almost maintained around 0.36 mg/min at the applied current at 0.5 A for a 25 h working period, illustrating the ideal durability of the HABDD. The free-standing HABDD electrode is suitable for O_3 generation from H_2O electrolysis under high-power operation [11].

The electrolytic reactions involving ozone production on diamond electrodes proceed as follows [11]:

$$2H_2O \rightarrow O_2 + 4H^+ + 4e^- \ (E^0 = 1.23\ V) \quad (1)$$

$$3H_2O \rightarrow O_3 + 6H^+ + 6e^- \ (E^0 = 1.51\ V) \quad (2)$$

$$H_2O + O_2 \rightarrow O_3 + 2H^+ + 2e^- \ (E^0 = 2.07\ V) \quad (3)$$

Oxygen (O_2) evolution will take place with a higher potential on the diamond electrode (1), which is thermodynamically preferred at E^0 = 1.23 V. O_3 is produced through reactions (2) and (3) with the O_2 evolution by reaction (1). Even if they are not thermodynamic,

O_3 generation will occur more efficiently due to a large overpotential for oxygen evolution on diamond electrodes.

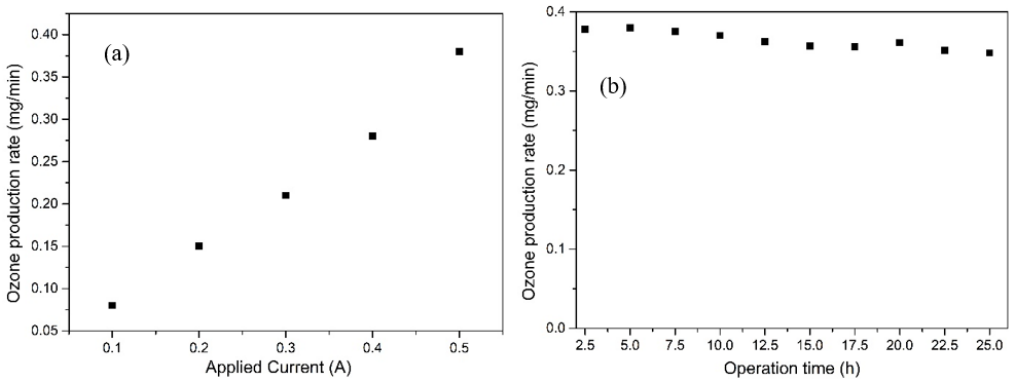

Figure 4. Ozone production rate depending on (**a**) the applied current, and (**b**) operation time at applied current of 0.5 A (Each production rate is represented as ■ in the Figure).

2.4. Photocatalysis Reactions

The main reactions in $TiO_2/O_3/UV$ photocatalysis include the following reaction paths [14].

$$TiO_2 + h\upsilon \rightarrow e^- + h^+ \quad (4)$$

$$H_2O + h^+ \rightarrow O\cdot + H^+ \quad (5)$$

$$O_3 + e^- \rightarrow O_3\cdot^- \quad (6)$$

$$O_3{}^- + H^+ \rightarrow HO_3 \quad (7)$$

$$HO_3\cdot \rightarrow OH\cdot + O_2 \quad (8)$$

$$O_3 + h\upsilon \rightarrow O\cdot + O_2 \quad (9)$$

$$O\cdot + H_2O \rightarrow 2OH \quad (10)$$

$$O_3 + OH\cdot \rightarrow HO_2\cdot + O_2 \quad (11)$$

Hydroxyl radicals (OH·) and other reactive oxygen species (ROS) generated on the TiO_2 surface are the main active species responsible for the degradation of organics in wastewater by advanced oxidation processes (AOPs). It should be noted TiO_2 nanotube growth on the Ti mesh structure is favorable for the adsorption of UV energy. The synergetic $TiO_2/O_3/UV$ method is an ideal AOP method for waste degradation in air or water. Under UV irradiation, the photo-generated electrons (in the conduction band, CB) and holes (in the valence band, VB) are separated in TiO_2 (4), which are captured by H_2O and O_3 molecules on the TiO_2 surface to form more active radicals such as OH· to attack the organics in water (5)–(8) (Figure 5a). Besides the decomposition of organics via the reactions (9)–(11) by O_3 individually, O_3 on the TiO_2 surface can trap the photo-generated electrons, thus effectively suppressing the recombination of the charge carrier pairs. In this case, more OH· and other ROS radicals will be generated by the synergetic effect from the $TiO_2/O_3/UV$ system. In the continuous flowing mode, the ROS radicals are formed in a dynamic balance.

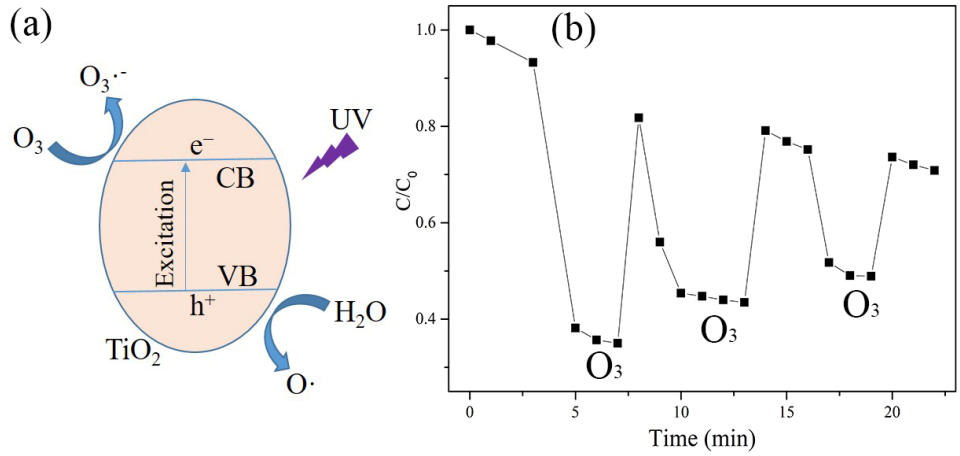

Figure 5. (**a**) Schematic illustration of O_3 molecules reaction on TiO_2 surface in water at UV activation. Electrons and holes are generated and separated under UV energy excitation. Electrons are injected into the CB and react with O_3 molecules, while holes are left in the VB and react with H_2O molecules; (**b**) Degradation of diclofenac (10 mg/L) in the TiO_2 photocatalysis upon O_3 response (Each concentration for monitoring is represented as ■ in the Figure).

The diclofenac removal efficiency upon the response to O_3 on TiO_2 photocatalysis was tested by discontinuous supplying of O_3, and the result is presented in Figure 5b. It can be seen O_3 assistance plays an important role in the organics degradation rate of TiO_2 photocatalysis. Besides absorbing UV energy, TiO_2 nanotubes could reflect the UV light among the microstructure and into the tap water, thus increasing the reaction probability of diclofenac with O_3. In comparison with the single TiO_2 photocatalysis process, the TiO_2/O_3/UV system improves the degradation efficiency due to its synergistic effect, both from the oxidation ability and charge separation assistance from O_3. This TiO_2/O_3/UV treatment system is able for the mineralization of pharmaceuticals with low concentrations in drinking water.

2.5. Diclofenac Degradation Efficiency

It is necessary for the evaluation of the degradation efficiency upon the mass transfer ability [15], which is in close relationship to the O_3 production efficiency. The photocatalytic degradation efficiency versus the electrolyte flowing rate is presented in Figure 6a. The highest removal efficiency was found at the flow rate of 150 mL/min on the HABDD surface. Initially, 10 min of photolysis with a 150 mL/min flow rate led to more than half degradation. This was because, on the one hand, under a lower flowing rate, the O_3 generation rate on the local area was increased while the total reaction rate was decreased due to a lower contact surface area at the interface of the electrode surface and the tap water. On the other hand, at a higher flowing rate, the tap water could not sufficiently contact the electrode surface before it flowed out. Hence, the flowing rate of the tap water should be selected at a moderate value.

The influence of the initial diclofenac concentration in the tap water was evaluated, and the result between 10 mg/L~100 mg/L is shown in Figure 6b. It was found the lower concentration (10 mg/L) had the highest removal efficiency than that with higher concentrations in 60 min of treatment. Organics with higher concentrations may be mass adsorbed on the TiO_2 surface, thus decreasing the photocatalytic activity. Diclofenac molecules at high concentrations also absorbed a considerable quantity of photons, thus leading to a decrease in the available photons absorbed by TiO_2. In addition, a higher amount of O_3 is required to completely decompose pharmaceuticals with higher concentrations. Concerning the practical concentration level of diclofenac is usually below 20 mg/L, this treatment can satisfy the requirement degradation needs. The heterogeneous reaction of the TiO_2 photocatalysis is affected by mass transfer from the O_3 molecules flowing to the catalyst

surface. An appropriate amount of O_3 enhances the TiO_2 photocatalytic activity, but excess O_3 will eliminate hydroxyl radicals by reaction (11).

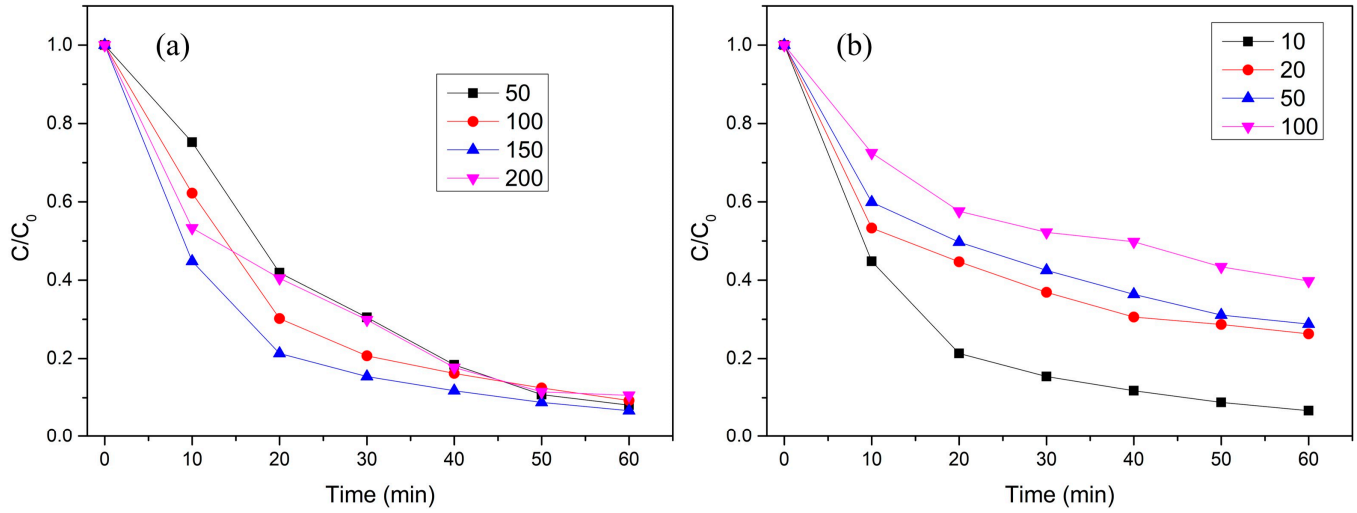

Figure 6. (**a**) Diclofenac concentration changes depending on the treatment time, flowing rate (50~200 mL/min), and (**b**) Initial concentration (10~100 mg/L) at flowing rate of 150 mL/min.

2.6. Ozone-Assisted TiO_2 Photocatalysis

In order to evaluate the ozone effect, different treatment routes upon the O_3 participation were compared. Diclofenac could be decomposed by TiO_2, O_3, or UV via five reaction paths [16], which include (a) UV, Direct photolysis of diclofenac by UV irradiation; (b) O_3, Direct oxidation of diclofenac by O_3; (c) O_3/UV, O_3 photocatalysis at the presence of H_2O (reaction 9); (d) TiO_2/UV, TiO_2 photocatalysis in aqueous solution; (e) TiO_2/O_3/UV, Synergistic photocatalysis in aqueous solution. The efficiency of these reaction paths followed the trend (e) > (c) > (d) > (b) > (a), as shown in Figure 7. The TiO_2/O_3/UV photocatalysis process showed the highest removal efficiency among these routes, which consumed 22.8 mg of O_3 to remove 85.56% diclofenac in tap water per hour. O_3 can react with organic compounds, and UV irradiation can accelerate the reaction rate [17]. Direct ozone attacks may take place on the amine group of organics [18]. In any case, ozonation assistance of diclofenac degradation is a fast reaction.

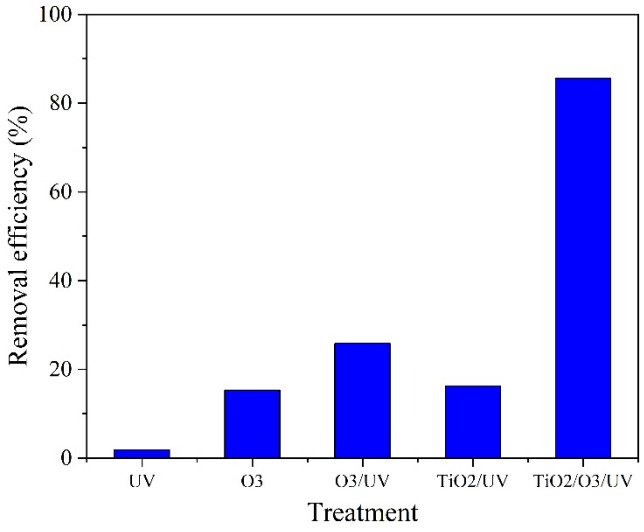

Figure 7. Comparison of removal efficiency of diclofenac by O_3, O_3/UV, TiO_2/UV, TiO_2/O_3/UV treatments in 1 h, the efficiency was calculated as $E = (C_0 - C)/C_0 \times 100\%$.

In this work, unlike other anticipation modes of O_3 into TiO_2 photocatalysis, the short diffusion distance of the O_3 molecule's travel paths improves the contact areas or reaction cross-section since O_3 generation from the HABDD surface to the TiO_2 surface. In addition, the mesh structure of the substrate provided good diffusion channels of organics and O_3 molecules in the TiO_2 nanotubes and improved the reflection efficiency of UV light. Under this circumstance, the reaction kinetic was increased due to the better diffusion pathways and pre-mixing effect in homogeneous conditions. Moreover, the reaction paths (a) (b) (c) together contribute to the TiO_2/O_3/UV photocatalysis more than their individual effect. Hence, the application of TiO_2/O_3/UV photocatalysis allowed almost complete removal of pharmaceuticals by ozonation and further mineralization of the by-products in the photocatalytic treatment [8].

Currently, the mainstream methods for photocatalytic degradation of diclofenac or other organics in water are normally based on oxides (TiO_2, MoS_2, ZnO, g-C_3N_4, etc.) nanoparticles dispersion in the aqueous media, achieving a highly heterogeneous catalysis efficiency. In general, more than 85% of diclofenac within 0.2 μg/L~10 mg/L could be removed at catalyst dose within 20 mg/L~1.5 g/L in 2 h in organics/catalysts mixtures [19–22]. Besides most photocatalysts are zero-dimensional nanomaterials, one-dimensional and two-dimensional nanostructures have been applied in diclofenac degradation in recent years [23,24]. Visible light or solar energy-driven photocatalytic degradation has attracted attention in future development [20,25,26]. In order to improve the removal performance, oxidants were introduced into photocatalysis to assist the oxidation and to expand the lifetime of the photo-generated holes and electrons [27]. The generation of more ROS plays an important role in increasing degradation efficiency [21,28]. Concerning the diclofenac concentration in this study was higher than many other methods, the removal efficiency of the TiO_2/O_3/UV system was satisfactory.

2.7. Theoretical Study on TiO_2/O_3 Interface

To further understand the synergistic effect of water-generated O_3 in the TiO_2 photocatalysis, the adsorption site and adsorption mode were studied by theoretical calculation. The final energy (single point energy) of different geometries and adsorption modes at the TiO_2/O_3 interface were calculated by the CASTEP (Cambridge serial total energy package, materials studio version 8.0). The single point energy is a measure of the electronic stability of a given atomic configuration and is typically used as a reference point for comparing the energies of different structures or for calculating thermodynamic properties such as enthalpy and entropy. The adsorption model in water is essential to investigate the adsorption behavior of O_3 molecules at the anatase TiO_2 (101) surface, which was constructed in a supercell (2 × 4 lattice) of anatase TiO_2 (101) lattice face with a slabbing thickness of ca. 5 Å. The lattice size of the adsorption model was built in 10.88 × 15.10 × 20.56 $Å^3$ volume, with the vacuum at 15 Å to avoid unnecessary inter-slab interactions. Surface water molecules (≡H_2O) and surface hydroxyl groups (≡OH) were chosen at the O_3 reaction sites. Bridging and side-armed configurations were regarded as effective linking ways for O_3 molecules to bind the reaction sites. Our simulations were constructed based on the generalized gradient approximation (GGA) of Perdew and Wang (PW91) calculations. The ultrasoft pseudopotentials were applied with a cutoff energy of 340 eV. The default Monkhorst–Pack was employed for the determination of k-points, and relaxation of the positions of all atoms was allowed.

As shown in Figure 8, the TiO_2 (101)/O_3 adsorption models have five maind adsorption models according to the simulation, named as (a) TiO_2≡$(H_2O)_2$-O_3 bridging, (b) TiO_2≡$(OH)_2$-O_3 bridging, (c) TiO_2≡H_2O-O_3 bridging, (d) TiO_2≡H_2O-O_3 single-armed, (e) TiO_2≡OH-O_3 single-armed, respectively. H_2O molecules or –OH species act as important linking bridges between O_3 molecules and TiO_2 surface, since they are linked in aqueous media.

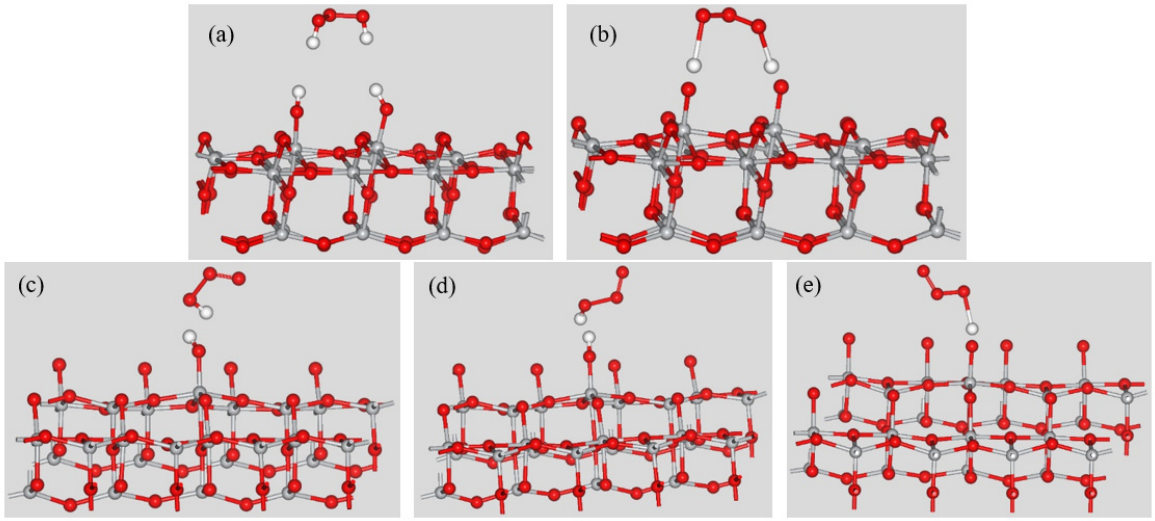

Figure 8. Illustration of TiO_2 (101)/O_3 adsorption models: (**a**) TiO_2≡$(H_2O)_2$-O_3 bridging, (**b**) TiO_2≡$(OH)_2$-O_3 bridging, (**c**) TiO_2≡H_2O-O_3 bridging, (**d**) TiO_2≡H_2O-O_3 single-armed, (**e**) TiO_2≡OH-O_3 single-armed.

The final energy (E_a) of O_3 molecules on the anatase TiO_2 (101) surface was calculated by the equation:

$$E_a = E_{ms} - E_m - E_s$$

where E_{ms} is the total energy of the TiO_2 surface with adsorbed O_3, E_m and E_s is the energy of the TiO_2 surface and O_3 molecules, respectively. The final energy of the adsorption mode is listed in Table 1. Both the exothermicity and stability in this interface system could be stable at a negative E_a value. The results illustrated that the bridging configuration (b) was more favorable for O_3 molecules adsorption in water than the other configuration, partly because the bridging mode (b) has a shorter average O-H binding length of 0.98 Å between the surface O atom and the H atom linking to the O_3 molecule. The Ti-O-H-O bridging mode benefits the photocatalysis reaction most since it can improve the separation efficiency of the photo-generated charges.

Table 1. Final energy of the adsorption mode.

Energy (eV)	a	b	c	d	e
E_{ms}	−61,825.7	−61,798.6	−61,357.8	−61,357.7	−61,344.1
E_m	60,487.69	60,456.88	60,036.76	60,036.73	60,021.25
E_s	1337.362	1337.362	1320.758	1320.683	1320.683
E_a	−0.62541	−4.3352	−0.28652	−0.32541	−2.19725

The adsorption of O_3 molecules on the TiO_2 surface is a key step to determine the efficiency of ROS generation since O_3 conversion to ROS species occurs at the TiO_2/O_3 interface [29]. Side-arms and bridging configurations are considered favorable styles for O_3-TiO_2 binding. Hydroxyl (-OH) groups and H_2O molecules on the surface are the dominant sites for the interaction with O_3 molecules since the reactions occur in aqueous media. Enhanced O_3 adsorption at the TiO_2 surface plays an important role in promoting heterogeneous catalysis performance.

3. Materials and Methods

Diclofenac as sodium salt was purchased from Sigma-Aldrich and directly used without further treatment. Tap water was obtained from the Chengdu Service Lines (Chengdu, China) and was purified by a Milli-Q system before use. Diclofenac aqueous

solution was prepared by direct dissolving in tap water at room temperature. Trimethyl borate ($B(OCH_3)_3$) was bought from Sigma Aldrich. Ti mesh was obtained from ChangTi Metal Co. (Shenzhen, China) and washed with ethanol before use.

The HABDD free-standing film was costume made by Zhengyinghao Metal Co. (Hefei, China) and was prepared using a microwave plasma-assisted chemical vapor deposition (MPCVD, 2.45 GHz) device. A Ta plate (10×10 cm^2) with arrayed holes was used as the deposition substrate for the diamond growth. Acetone and hydrogen gas mixture was used as the carbon source in the deposition. Trimethyl borate as the boron doping agent was mixed into the carrier gas (boron doping affords the conductivity of synthetic diamond). Both sides of the Ta substrate were exposed for the diamond growth in sequence. TiO_2 nanotubes on the Ti mesh were synthesized by electrochemical anodization treatment according to our past works [30]. Briefly, the Ti mesh was used as the working electrode, and a Pt plate as the counter electrode. The anodization reaction was performed in an electrolyte containing formamide (94.7 wt%), H_2O (4.4 wt%), and NH_4F (0.9 wt%) for 20 h treatment.

The electrochemical-photocatalytic system for the degradation of diclofenac in tap water is schematically illustrated in Figure 1. The reactor was made of Pyrex glass to observe the reaction state. This electrochemical part was composed of the HABDD anode (4×4 cm^2) and a platinum mesh cathode that separated by Nafion films (DuPont, Wilmington, DE, USA), which were also used as the solid-state electrolyte membrane. On the cathodic side, hydrogen was produced on the Pt electrode and was carried out by the flowing tap water. In the photocatalysis part, the as-obtained TiO_2 nanotube film (4×4 cm^2) was parallel placed adjacent to the HABDD and illuminated by an incident UV lamp (254 nm, Atlantic Ultraviolet Co., Hauppauge, NY, USA) behind. The distance between the TiO_2 nanotubes and the HABDD surface was 2 cm. The degradation treatment was conducted in a continuous flowing mode with diclofenac-containing tap water inlet and water outlet channels circulated by a pump. The diclofenac-containing tap water streamed in a screw-like fluent through the TiO_2 photocatalyst in circulation driven by the pump from an external reservoir tank.

The surface morphologies of the samples were examined by scanning electron microscope (SEM, JSM-5400, JEOL). The phase of the TiO_2 nanotube sample was characterized by X-ray diffraction (XRD, Rigaku RINT1500). The BET was measured by physisorption analyzer (ASAP 2460). The diclofenac concentration was measured by high-performance liquid chromatography (HPLC, Varian 940) with a photodiode array detector. Samples were taken at interval time for HPLC analysis. Ozone dissolved in the tap water was on-line monitored by a table ozone detector (PGD3-C, Xinhairui Co. Shenzhen, China), which was calibrated by laboratory instrument before use.

4. Conclusions

TiO_2 nanotubes fabricated on a Ti mesh were used as the photocatalyst in combination with O_3 for the degradation of diclofenac in tap water. An HABDD electrode was used to electrochemically generate O_3, which created almost in situ ozone-feeding channels to assist the TiO_2 photocatalysis. The study investigated the effect of O_3 generation rate, diclofenac removal performance, treatment time, flowing rate, and initial concentration of diclofenac on the degradation efficiency. The $TiO_2/O_3/UV$ photocatalysis system was found to be more effective than other methods, such as UV, O_3, O_3/UV, and TiO_2/UV, due to its synergetic efficiency. Additionally, the nanostructure of TiO_2 and the mesh microstructure optimized the diffusion pathways for O_3 molecules and organics onto the photocatalyst surface. The study also estimated the O_3 adsorption capability on the TiO_2 (101)/O_3 interface and suggested that O_3 assistance is an effective method for enhancing the decomposition rate of organics. Overall, the synergetic $TiO_2/O_3/UV$ photocatalysis system shows promise for the treatment of tap water and wastewater containing pharmaceuticals.

Author Contributions: Methodology, Software, writing, D.M.; Resources, investigation, X.H.; Software, formal analysis, X.L.; Conceptualization, writing—review and editing D.L. All authors have read and agreed to the published version of the manuscript.

Funding: This research was funded by the funding from Science & Technology Department of Sichuan Province (2022NSFSC0314 and 2023NSFSC0633), the Fundamental Research Funds for the Central Universities (2022), the R&D Program of Beijing Municipal Education Commission (KM202310017003), and the Experimental Technology Project of Sichuan University (SCU201204, SCU201207, SCU1096).

Data Availability Statement: The data that support the finding of this study are available from the corresponding author upon reasonable request.

Acknowledgments: The authors thank the technical support from Shuguang Yan from Analytical & Testing Center, Sichuan University.

Conflicts of Interest: The authors declare no conflict of interest.

References

1. Paumo, H.K.; Dalhatou, S.; Katata-Seru, L.M.; Kamdem, B.P.; Tijani, J.O.; Vishwanathan, V.; Kane, A.; Bahadur, I. TiO_2 assisted photocatalysts for degradation of emerging organic pollutants in water and wastewater. *J. Mol. Liq.* **2021**, *331*, 115458. [CrossRef]
2. He, Y.J.; Sutton, N.B.; Rijnaarts, H.H.H.; Langenhoff, A.A.M. Degradation of pharmaceuticals in wastewater using immobilized TiO_2 photocatalysis under simulated solar irradiation. *Appl. Catal. A -Environ.* **2016**, *182*, 132–141. [CrossRef]
3. Kanakaraju, D.; Motti, C.A.; Glass, B.D.; Oelgemöller, M. Photolysis and TiO_2-catalysed degradation of diclofenac in surface and drinking water using circulating batch photoreactors. *Environ. Chem.* **2014**, *11*, 51–62. [CrossRef]
4. Montoya-Bautista, C.V.; Avella, E.; Ramírez-Zamora, R.-M.; Schouwenaas, R. Metallurgical wastes employed as catalysts and photocatalysts for water treatment: A review. *Sustainability* **2019**, *11*, 2470. [CrossRef]
5. García-Araya, J.F.; Beltrán, F.J.; Aguinaco, A. Diclofenac removal from water by ozone and photolytic TiO_2 catalysed processes. *J. Chem. Technol. Biotechnol.* **2010**, *85*, 798–804. [CrossRef]
6. Li, L.S.; Zhang, P.Y.; Zhu, W.P.; Han, W.Y.; Zhang, Z.L. Comparison of O_3-BAC, UV/O_3-BAC and TiO_2/UV/O_3-BAC processes for removing organic pollutants in secondary effluents. *J. Photoch. Photobiol. A* **2005**, *171*, 145–151. [CrossRef]
7. Dutschke, M.; Schnabel, T.; Schütz, F.; Springer, C. Degradation of chlorinated volatile organic compounds from contaminated ground water using a carrier-bound TiO_2/UV/O_3-system. *J. Environ. Manag.* **2022**, *304*, 114236. [CrossRef] [PubMed]
8. Márquez, G.; Rodríguez, E.M.; Maldonado, M.I.; Álvarez, P.M. Integration of ozone and solar TiO_2-photocatalytic oxidation for the degradation of selected pharmaceutical compounds in water and wastewater. *Sep. Purif. Technol.* **2014**, *136*, 18–26. [CrossRef]
9. Sahle-Demessie, E.; Devulapelli, V.G. Oxidation of methanol and total reduced sulfur compounds with ozone over V_2O_5/TiO_2 catalyst: Effect of humidity. *Appl. Catal. A -Gen.* **2009**, *361*, 72–80. [CrossRef]
10. Zhang, P.; Liang, F.; Yu, G.; Chen, Q.; Zhu, W. A comparative study on decomposition of gaseous toluene by O_3/UV, TiO_2/UV and O_3/TiO_2/UV. *J. Photochem. Photobio. A Chem.* **2003**, *156*, 189–194.
11. Fujishima, A.; Einaga, Y.; Rao, T.N.; Tryk, D.A. *Diamond Electrochemistry*; BKC INC.: Tokyo, Japan; Elsevier B. V.: Amsterdam, The Netherlands, 2005; ISBN 0-444-51908-4/4-939051-33-1.
12. Luo, D.B.; Ma, D.C.; Wu, L.Z.; Zhi, J.F. A high-performance wastewater treatment system for orange II degradation using a boron-doped diamond electrode and enhanced by zeolite-TiO_2 photocatalyst. *Int. J. Electrochem. Sci.* **2018**, *13*, 5904–5922. [CrossRef]
13. Suzuki, N.; Okazaki, A.; Takagi, K.; Serizawa, I.; Okada, G.; Terashima, C.; Katsumata, K.; Kondo, T.; Yuasa, M.; Fujishima, A. Formation of ammonium ions by electrochemical oxidation of urea with a boron-doped diamond electrode. *New J. Chem.* **2020**, *44*, 17637–17640. [CrossRef]
14. Qi, H.; Sun, D.Z.; Chi, G.Q. Formaldehyde degradation by UV/TiO_2/O_3 process using continuous flow mode. *J. Environ. Sci.* **2007**, *19*, 1136–1140. [CrossRef]
15. Fukinbara, S.; Shiraishi, F. Characteristics of the photocatalytic reactor with an annular array of glass tubes surrounding a light source. 2. Kinetic analysis. *CELSS J.* **2001**, *13*, 11–23.
16. Lu, S.Y.; Wang, Q.L.; Buekens, A.G.; Yan, J.H.; Li, X.D.; Cen, K.F. Photocatalytic decomposition of gaseous 1,2-dichlorobenzene on TiO_2 films: Effect of ozone addition. *Chem. Engin. J.* **2012**, *195–196*, 233–240. [CrossRef]
17. Huber, M.M.; Gobel, A.; Joss, A.; Hermann, N.; Loffler, D.; McArdell, C.S.; Ried, A.; Siegrist, H.; Ternes, T.A.; Gunten, U.v. Oxidation of pharmaceuticals during ozonation of municipal wastewater effluents: A pilot study. *Environ. Sci. Technol.* **2005**, *39*, 4290–4299. [CrossRef] [PubMed]
18. Huber, M.M.; Canonica, S.; Park, G.Y.; Gunten, U.V. Oxidation of pharmaceuticals during ozonation and advanced oxidation processes. *Environ. Sci. Technol.* **2003**, *37*, 1016–1024. [CrossRef]
19. Irandost, M.; Akbarzadeh, R.; Pirsaheb, M.; Asadi, A.; Mohammadi, P.; Sillanpää, M. Fabrication of highly visible active N, S co-doped TiO_2@MoS_2 heterojunction with synergistic effect for photocatalytic degradation of diclofenac: Mechanisms, modeling and degradation pathway. *J. Mol. Liq.* **2019**, *291*, 111342. [CrossRef]

20. Rueda-Salaya, L.; Hernández-Ramírez, A.; Hinojosa-Reyes, L.; Guzmán-Mar, J.L.; Villanueva-Rodríguez, M.; Sánchez-Cervantes, E. Solar photocatalytic degradation of diclofenac aqueous solution using fluorine doped zinc oxide as catalyst. *J. Photoch. Photobiol. A* **2020**, *391*, 112364. [CrossRef]
21. You, Q.L.; Zhang, Q.X.; Gu, M.B.; Du, R.J.; Chen, P.; Huang, J.; Wang, Y.J.; Deng, S.B.; Yu, G. Self-assembled graphitic carbon nitride regulated by carbon quantum dots with optimized electronic band structure for enhanced photocatalytic degradation of diclofenac. *Chem. Eng. J.* **2022**, *431*, 133927. [CrossRef]
22. Padervand, M.; Rhimi, B.; Wang, C.Y. One-pot synthesis of novel ternary $Fe_3N/Fe_2O_3/C_3N_4$ photocatalyst for efficient removal of rhodamine B and CO_2 reduction. *J. Alloys Compd.* **2021**, *852*, 156955. [CrossRef]
23. Bai, X.J.; Guo, L.L.; Jia, T.Q.; Hao, D.; Wang, C.; Li, H.Y.; Zong, R.L. Perylene diimide growth on both sides of carbon nanotubes for remarkably boosted photocatalytic degradation of diclofenac. *J. Hazard. Mater.* **2022**, *435*, 128992. [CrossRef]
24. Dekkouche, S.; Morales-Torres, S.; Ribero, A.R.; Faria, J.L.; Fontàs, C.; Kebiche-Senhadji, O.; Silva, A.M.T. In situ growth and crystallization of TiO_2 on polymeric membranes for the photocatalytic degradation of diclofenac and 17α-ethinylestradiol. *Chem. Eng. J.* **2022**, *427*, 131476. [CrossRef]
25. Liu, W.; Li, Y.Y.; Liu, F.Y.; Jiang, W.; Zhang, D.D.; Liang, J.L. Visible-light-driven photocatalytic degradation of diclofenac by carbon quantum dots modified porous g-C_3N_4: Mechanisms, degradation pathway and DFT calculation. *Water Res.* **2019**, *151*, 8–19. [CrossRef] [PubMed]
26. Padervand, M.; Hajiahmadi, S. Ag/AgCl@Tubular g-C_3N_4 nanostructure as an enhanced visible light photocatalyst for the removal of organic dye compounds and biomedical waste under visible light. *J. Photoch. Photobiol. A* **2022**, *425*, 113700. [CrossRef]
27. Martínez, C.; Fernández, M.I.; Santaballa, J.A.; Faria, J. Aqueous degradation of diclofenac by heterogeneous photocatalysis using nanostructured materials. *Appl. Catal. B -Environ.* **2011**, *107*, 110–118. [CrossRef]
28. Chen, P.; Zhang, Q.X.; Su, Y.H.; Shen, L.Z.; Wang, F.L.; Liu, H.J.; Liu, Y.; Cai, Z.W.; Lv, W.Y.; Liu, G.G. Accelerated photocatalytic degradation of diclofenac by a novel CQDs/BiOCOOH hybrid material under visible-light irradiation: Dechloridation, detoxicity, and a new superoxide radical model study. *Chem. Eng. J.* **2018**, *332*, 737–748. [CrossRef]
29. Li, X.Y.; Shen, Z.; Zhang, H.; Li, X.Y.; Zhou, Y.J.; Yao, H. Insights into enhanced O_3 adsorption on Ti/ anatase TiO_2 (101) surfaces by positive electric Fields: A theoretical exploration. *Chem. Eng. J.* **2022**, *440*, 135665. [CrossRef]
30. Luo, D.B.; Liu, B.S.; Fujishima, A.; Nakata, K. TiO_2 nanotube arrays formed on Ti meshes with periodically arranged holes for flexible dye-sensitized solar cells. *ACS Appl. Nano Mater.* **2019**, *2*, 3943–3950. [CrossRef]